IBIC 2021
International Beam Instrumentation Conference

Development of a Pass-through Diagnostic for Next-generation XFELs Using Diamond Detectors

SLAC NATIONAL ACCELERATOR LABORATORY

I. Silva Torrecilla†, B. Jacobson, J. MacArthur, D. Zhu, SLAC National Accelerator Laboratory, Menlo Park, California, USA
J. Bohon, D. Kim, J. Smedley, Los Alamos National Laboratory, Los Alamos, New Mexico, USA
E. Gonzalez, S. Kachiguine, F. Martinez-Mckinney, S. Mazza, M. Nizam, N. Norvell, R. Padilla, E. Potter, E. Ryan, B. Schumm, M. Tarka, M. Wilder, Santa Cruz Institute for Particle Physics and the University of California at Santa Cruz, Santa Cruz, California, USA
C. T. Harris, Sandia National Laboratory, Albuquerque, New Mexico, USA

Abstract

X-ray FELs deliver rapid pulses on the femtoseconds scale, and high peak intensities that fluctuate strongly on a pulse-to-pulse basis. The fast drift velocity, and high radiation tolerance properties of CVD (chemical vapor deposition) diamonds, make these crystals a good candidate material for developing a multi-hundred MHz pass-through diagnostic for the next generation of XFELs. Commercially available diamond sensors work as position-sensitive pass-through diagnostics for nJ-level pulses from synchrotrons. Supported by the University of California and the SLAC National Laboratory, a collaboration of UC campuses and National Laboratories have developed a new approach to the readout of diamond diagnostic sensors designed to facilitate operation for FEL-relevant uJ and mJ pulses. Single-crystal diamond detectors have been tested on the XPP end station of the Linac Coherent Light Source beam at SLAC. We present results on the linearity and charge collection characteristics as a function of the density of deposited charge.

Research

Sydor Commercial Board with Diamond Sensor

Readout Scheme

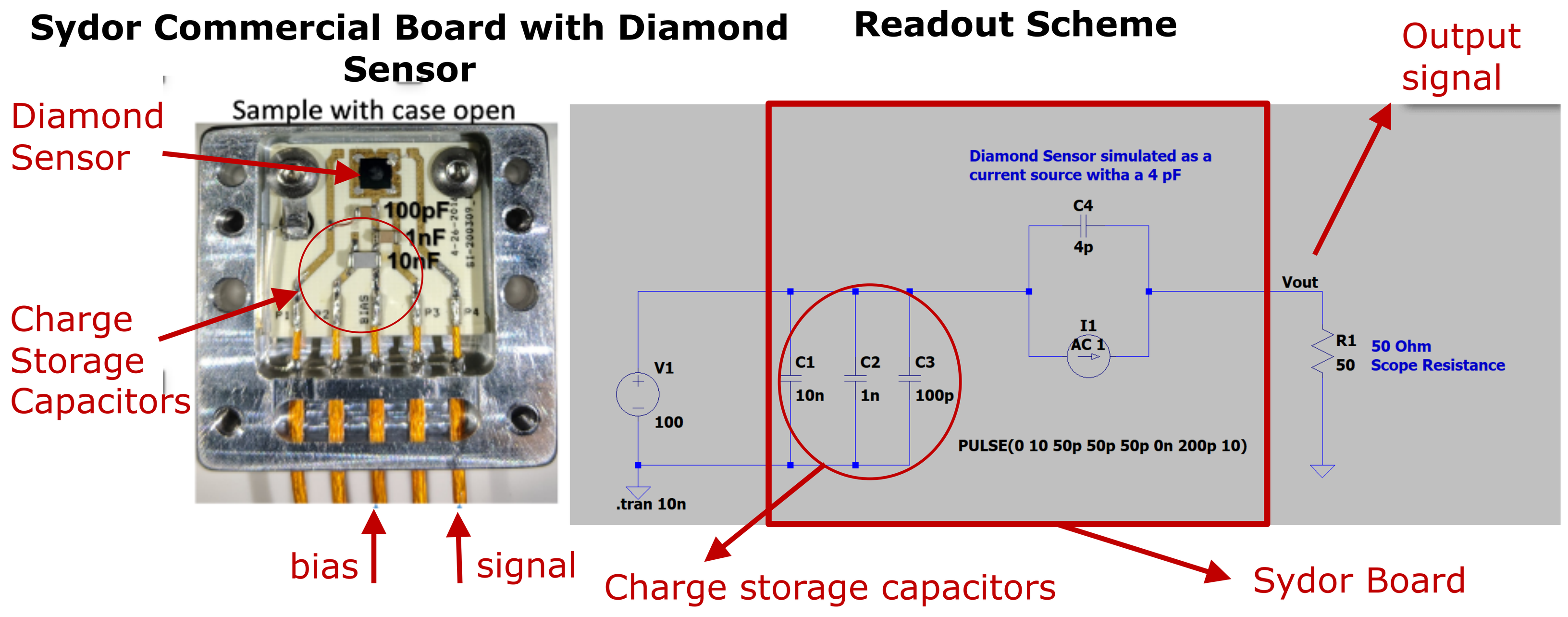

- 500 µm thickness diamond sensor with a 4pF capacitance
- Charge storage capacitors C1,C2, & C3 which quickly supply of charge to the sensor
- Output signal channeled directly through a 50 Ohm Oscilloscope
- 10 uJ of absorbed energy in 100 ps will generate a current of 10^4 A; generating a voltage across the 50 Ohm resistor of 5×10^5 V. If the rate change dI/dt encounters a stray inductance of 10 nH, this will generate a back EMF voltage of about 1.0×10^6 V.
- This will un-bias the sensor and stop the charge collection

Reference: https://sydortechnologies.com/x-ray-beam-monitors/

Diamond Sensor with Pt electrodes (SCIPP board)

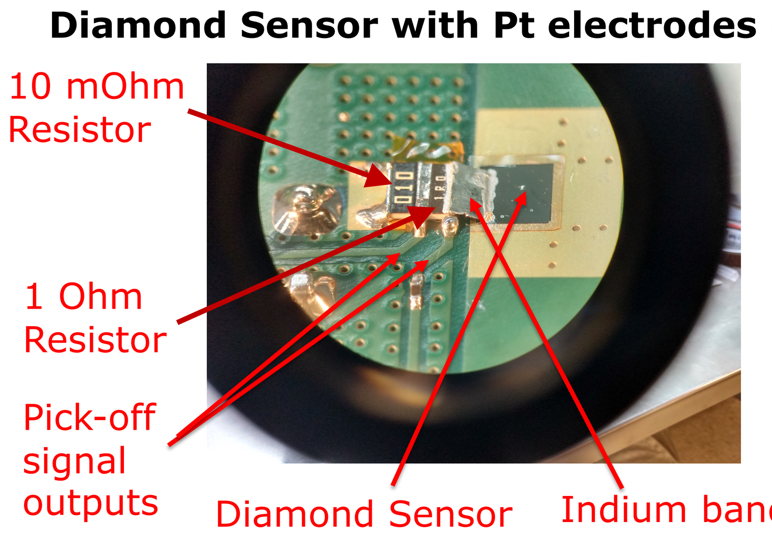

- 37 um thickness diamond sensor shown, also have a 500 um thick diamond
- In order to reduce inductance effects no bond wires were used to connect the components of the circuit
- Instead, an Indium band connects the sensor to the readout chain

SCIPP Readout Board Scheme

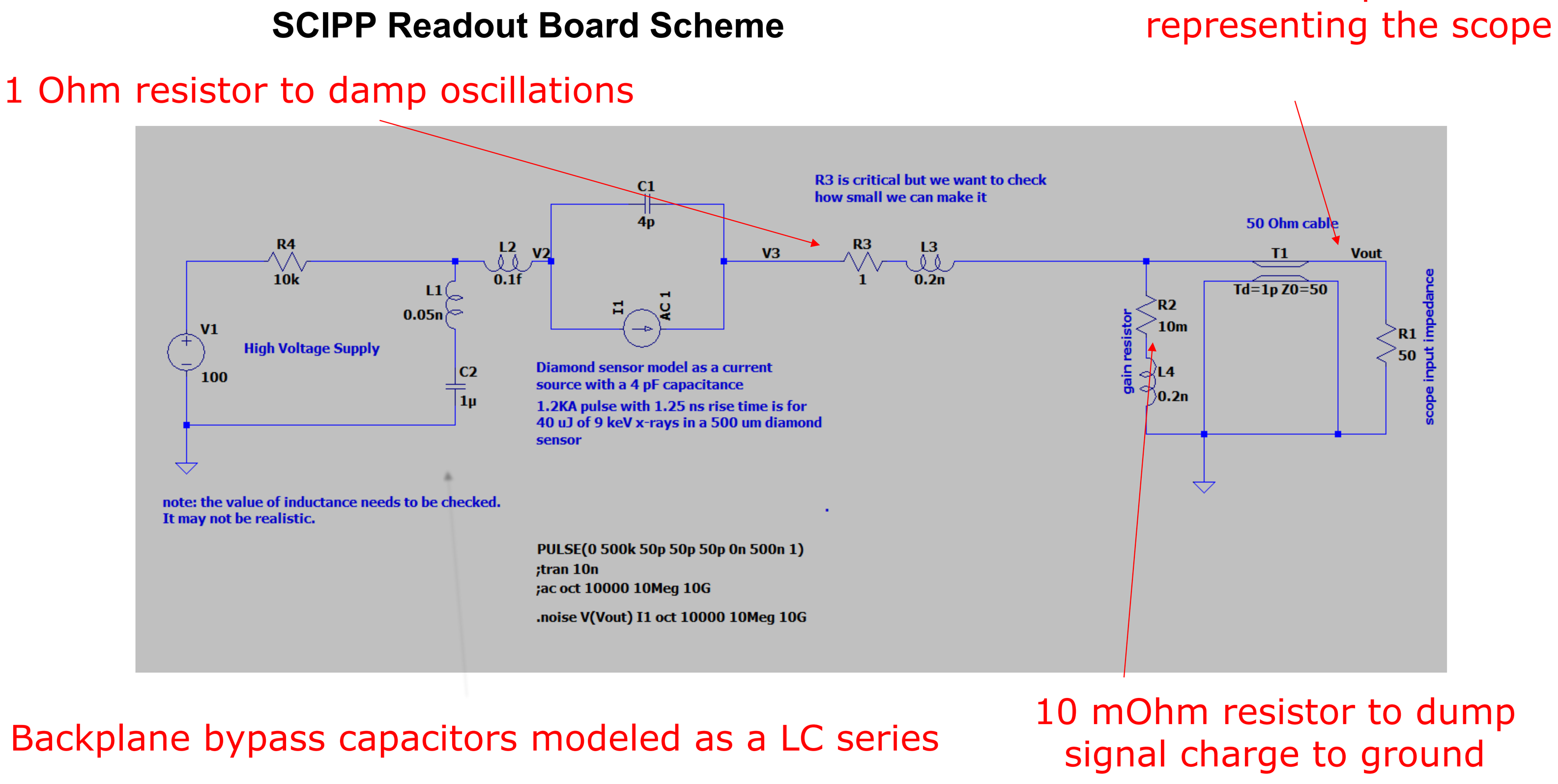

- R4 is a 10k resistor to limit a current in the event of a short on the board, and part of the RC low pass filter.
- C2 represents a bank of bypass capacitors in parallel to reduce inductance and to quickly supply of charge to the sensor
- R3 is a damping oscillation resistor
- R2 is a 10 mOhm to dump most of the current and avoid damaging our scope
- 10 uJ of absorbed energy in 100ps will generate a current of 10^4 A.

Diamond Sensor Properties

- Density 3.51 g/cm^3
- Drift Velocity saturates at 5V/um at 200 um/nsec
  - For saturated 500 µm sensor charge collected in 2.5 ns
  - For saturated 20 µm sensor charge collected in 100 ps
- Energy bandgap 5.5 eV
- Electron/hole rate at 13.3 eV/ion-pair
- Expected to be highly radiation resistance
- Diamond offers fast drift velocity and (expected) radiation tolerance

Results

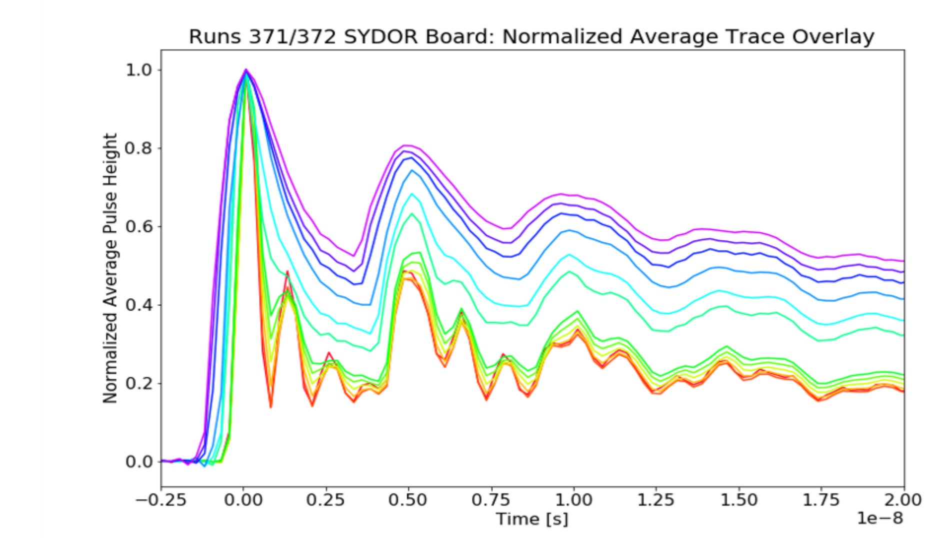

Average traces for a sensor using the Sydor commercial board. Data taken November 2020

Diamond Detectors Test at XPP end station at LCLS XFEL. April 6th, 2021

- Monochromatic beam of 11.89 keV X-rays with individual pulse varying from a fraction of a µJ to energies in excess of 80 µJ
- Data was accumulated with both the full beam as well as with a beam attenuated by 90% through the insertion of a physical attenuator upstream of the sensor assembly

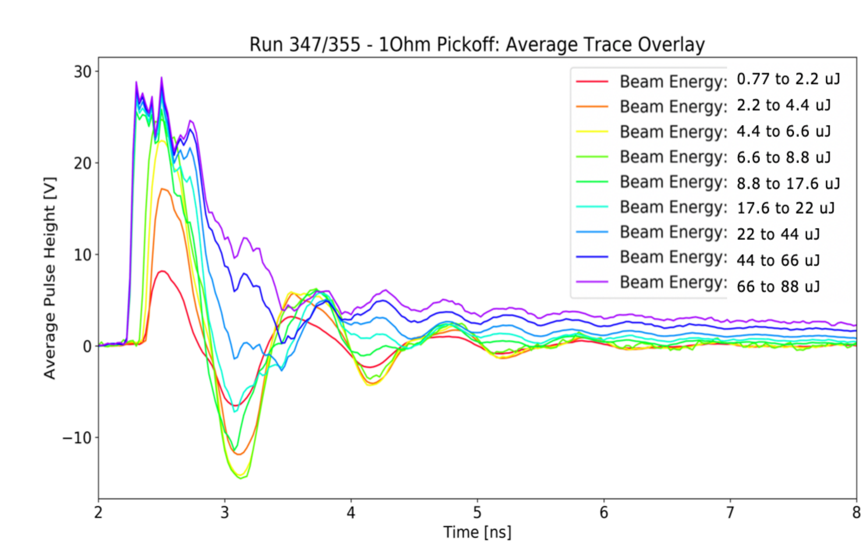

Average traces for a sensor bias at 100 V using the SCIPP board

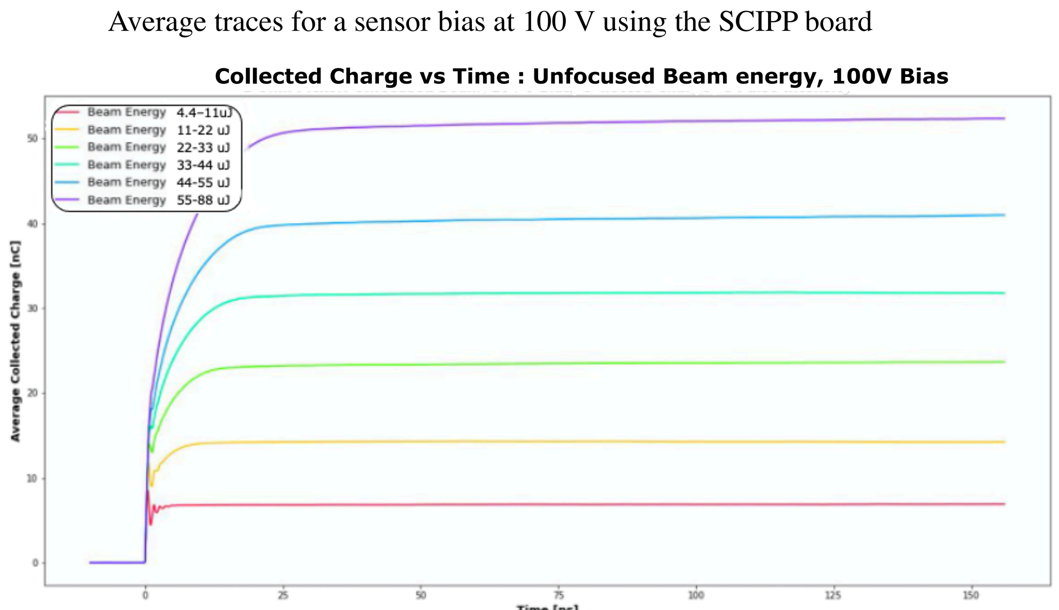

Collected charge as a function of collection time for a sensor bias of 100 V, with the beam focused to a FWHM of 350 μm.

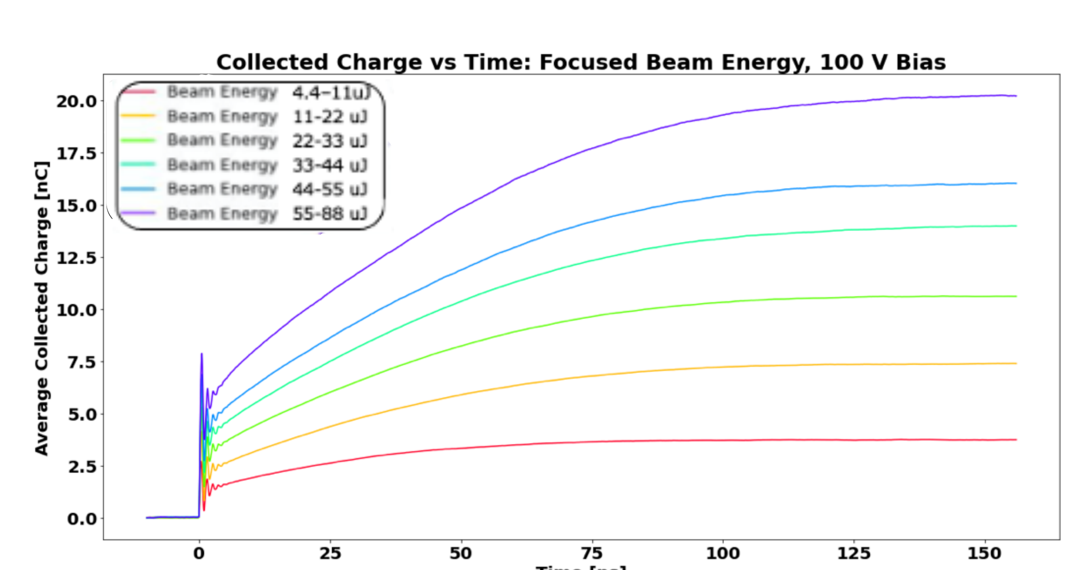

Collected charge as a function of collection time for a sensor bias of 100 V, with the beam focused to a FWHM of 43 μm.

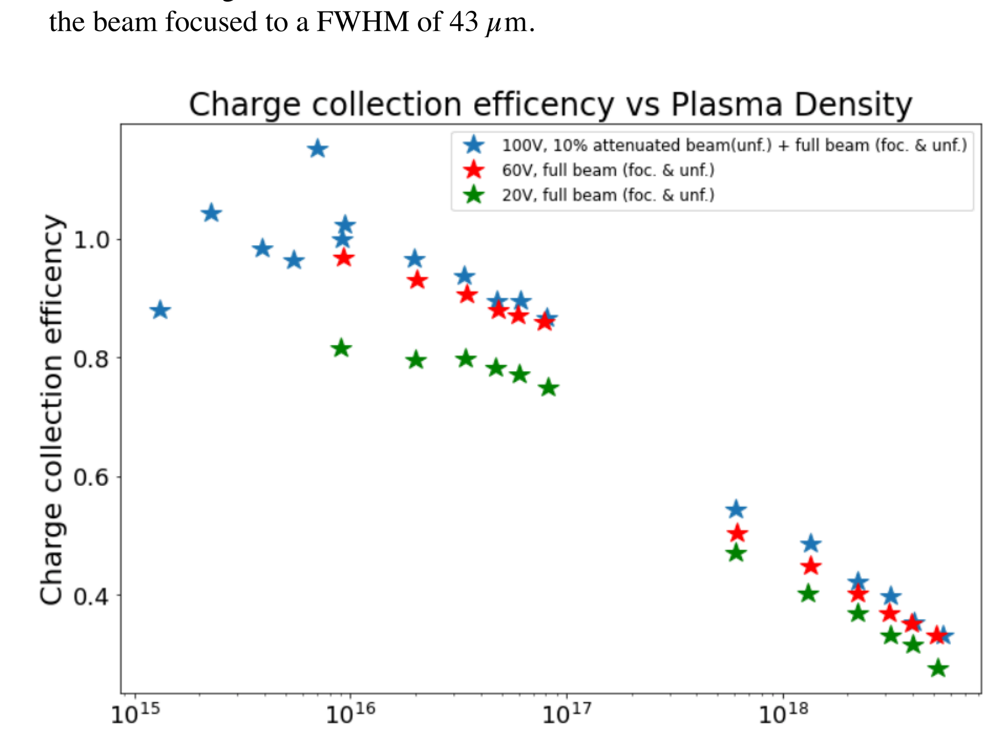

Estimated charge collection efficiency as a function of plasma density (cm^{-3}) for 100 V, 60 V and 20 V sensor bias.

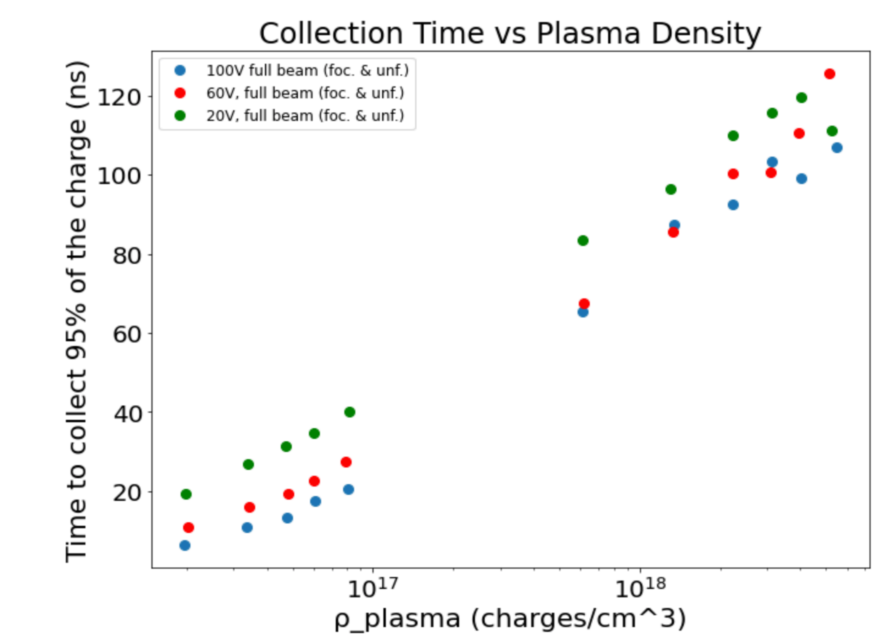

Time required to collect 95% of $Q_{coll}(t\rightarrow\infty)$, as a function of plasma density, for various detector biasing levels.

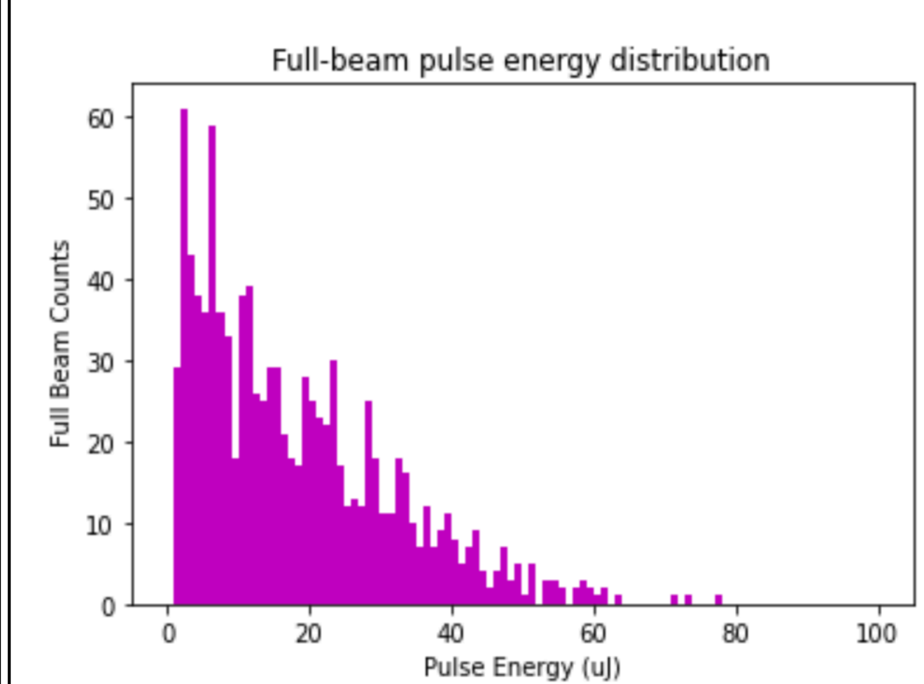

Typical distribution of pulse energies delivered by the LCLS during data accumulation.

Charge collection efficiency table at 100V bias

Average Energy [uJ]	Efficency	Plasma density
Unfocused Beam		
7.4074	0.999990255	9.19E+15
15.84	0.966810579	1.96E+16
27.06	0.938187098	3.36E+16
38.192	0.895645979	4.74E+16
49.06	0.895398004	6.08E+16
64.768	0.867424791	8.03E+16
Focused Beam		
7.392	0.543334929	6.07E+17
16.346	0.48760216	1.34E+18
27.17	0.423338064	2.23E+18
38.258	0.397621566	3.14E+18
48.994	0.355382815	4.03E+18
66.682	0.331400086	5.48E+18
10% attenuated unfocused beam		
0.9108	0.878876332	1.30E+15
1.5818	1.042680681	2.27E+15
2.728	0.984274895	3.91E+15
3.806	0.963522859	5.45E+15
4.884	1.150369887	6.99E+15
6.556	1.023008725	9.39E+15

Conclusions

- For highest bias voltage, charge collection efficiency was found to be maintained for plasma densities as high as 10^{16} cm^{-3}. The charge collection efficiency worsened monotonically with applied bias voltage
- Charge collection time, characterized by the amount of time required to accumulate 95% of the asymptotic value of collected charge, was also found to depend strongly on plasma density and detector bias voltage.
- The results suggest that the intrinsic charge collection properties of monocrystalline diamond will present challenges to the development of pass-through diagnostics for high-intensity XFEL beams (which can approach several mJ), especially for high repetition-rate applications.

Acknowledgments

This work was performed, in part, at the Center for Integrated Nanotechnologies, an Office of Science User Facility operated for the U.S. Department of Energy (DOE) Office of Science by Los Alamos National Laboratory (Contract 89233218CNA000001) and Sandia National Laboratories (Contract DE-NA-0003525).

Use of the Linac Coherent Light Source (LCLS), SLAC National Accelerator Laboratory, is supported by the U.S. Department of Energy, Office of Science, Office of Basic Energy Sciences under Contract No. DE-AC02-76SF00515.